Theor. Appl. Climatol. 66, 13–27 (2000)

Theoretical and Applied Climatology

[1] Institute of Atmospheric Physics, Prague, Czech
[2] Department of Meteorology and Environment Protection, Charles University, Prague, Czech

Constructing Site-Specific Climate Change Scenarios on a Monthly Scale Using Statistical Downscaling

R. Huth[1] and **J. Kyselý**[1,2]

With 11 Figures

Received December 3, 1998
Revised December 4, 1999

Summary

Monthly mean temperature and monthly precipitation totals in two small catchments in the Czech Republic are estimated from large-scale 500 hPa height and 1000/500 hPa thickness fields using statistical downscaling. The method used is multiple linear regression. Whereas precipitation can be determined from large-scale fields with some confidence in only a few months of the year, temperature can be determined successfully. Principal components calculated separately from the height and thickness anomalies are identified as the best predictor set. The method is most accurate if the regression is performed using seasons based on three months. The test on an independent sample, consisting of warm seasons, confirms that the method successfully reproduces the difference in mean temperature between two climatic states, which indicates that this downscaling method is applicable for constructing scenarios of a future climate change. The ECHAM3 GCM is used for scenario construction. The GCM is shown to simulate surface temperature and precipitation with low accuracy, whereas the large-scale atmospheric fields are reproduced well; this justifies the downscaling approach. The observed regression equations are applied to $2xCO_2$ GCM output so that the model's bias is eleminated. This procedure is then discussed and finally, temperature scenarios for the $2xCO_2$ climate are constructed for the two catchments.

1. Introduction

It is recognized that there is a gap between what general circulation models (GCMs) can produce with reasonable levels of confidence and what is required for climate change impact studies (von Storch, 1995; Kattenberg et al., 1996). Methods of bridging this gap, that is, of translating the most reliable GCM output to the surface variables, required at regional and local scales by impact researchers, are commonly referred to as downscaling techniques (Giorgi and Mearns, 1991). Specifically, statistical downscaling is based on seeking statistical relationships between sets of predictors (variables that are well represented by GCMs) and predictands (variables needed for impact studies). Starting from the pioneering paper by Kim et al. (1984), a variety of approaches to statistical downscaling have been employed which vary in their temporal and spatial scales, their statistical methods, and the variables included in the process.

GCMs simulate upper-air variables more accurately than the surface variables; large-scale fields are simulated better than values at a single gridpoint (gridbox) (Grotch and MacCracken, 1991; Gates et al., 1996). Therefore, large-scale upper-air variables are a good choice as predictors in downscaling studies. Furthermore, the predictors selected for downscaling must explain a sufficient portion of the variance of the predictands. Circulation variables (geopotential heights and sea level pressure) have therefore been used in many studies as the only predictor in downscaling variables, such as temperature and precipitation (von Storch et al., 1993; Hewitson, 1994; Corte-Real et al., 1995; Schubert and Henderson-Sellers, 1997). Changes in circulation do not appear to be the main source of observed long-term surface climate trends (Yarnal, 1985; Huth, 1999), and therefore, changes in surface climate due to the enhanced greenhouse effect as determined by downscaling GCM-simulated circulation alone, may not be reliable. The downscaling-from-circulation method fails, for example, in the simple case where the whole troposphere warms up in future climate whereas the circulation remains unchanged. A possible remedy to this problem suggested in recent studies, is to include among the predictors other large-scale fields that affect surface conditions, such as temperature in the free atmosphere (Kaas and Frich, 1995; Cavazos, 1997).

There are several unresolved issues in the application of statistical downscaling procedures to GCM output. They concern two topics: (i) the climatology from which the predictor and predictand anomalies in GCM climates (both in the control and perturbed runs) are calculated, and (ii) the way the principal components (PCs), representing the predictor field, are defined in the GCM output. In the majority of relevant studies, either the options are selected without a proper substantiation or the selected options are not explicitly mentioned at all.

This study aims to construct time series of monthly mean temperature and precipitation by downscaling outputs from the ECHAM3 GCM for a $2xCO_2$ climate situation in two small catchments in the Czech Republic. The emphasis is put on methodological considerations regarding the application of statistical downscaling to GCM output. The results of the study will be used to investigate climate change impacts on hydrological regimes in the two catchments. The data used in this study are described in Sec. 2 and the downscaling method is described in Sec. 3. Section 4 deals with GCM control run validation based on two points of view: 1. Is there a need for downscaling, i.e., are GCM-simulated temperatures and precipitation too unreliable for direct use in impact studies (cf. Palutikof et al., 1997)? 2. Are the large-scale fields simulated accurately enough to be used as predictors? In Sec. 5 the downscaling method is applied to observed data, concentrating on the selection of predictors and the optimum definition of seasons. The downscaling method is then applied to the control and $2xCO_2$ GCM output in Sec. 6 along with a discussion of the related methodological considerations. The time series of monthly values for a $2xCO_2$ climate (climate change scenario) are constructed and the results are summarized in Sec. 7.

2. Datasets

Thirty years of observations and thirty years of both control and equilibrium $2xCO_2$ experiments with the ECHAM3 GCM are used in this study. The ECHAM3 model has a T42 resolution, corresponding approximately to a 2.8° grid step both in longitude and latitude. In the control run, climatological SSTs and sea ice were employed while the $2xCO_2$ run was forced by SSTs and sea ice averaged over years 65 to 74 (roughly corresponding to doubling the CO_2 concentration) in the scenario A transient integration. Observations span the period 1961–1990; the GCM simulations span years 11 to 40 in the control run and 13 to 42 in the $2xCO_2$ run. A more detailed description of the ECHAM3 model can be found in DKRZ (1993).

Two large-scale predictors are considered. Upper-air circulation is represented by 500 hPa geopotential heights (Z500); temperature of the lower troposphere is characterized by 1000/500 hPa thickness (TH). The observed data are taken from NCEP reanalyses. They were interpolated from the original $5° \times 5°$ grid onto the model grid using bicubic splines. To reduce the amount of data, the grid is used with a halved resolution (approximately $5.6° \times 5.6°$) to represent predictor fields in both the observations and GCM output. The area of interest covers most of Europe and extends from 16.9° W to 28.1° E and from 32.1° N to 65.6° N, thereby consisting of 63 gridpoints.

The geographic location of the catchments of the Metuje and Blanice rivers is shown in Fig. 1. The precipitation series for the Metuje catchment were obtained by simply averaging data from five gauges; the precipitation series for the Blanice catchment and temperatures for both catchments consist of data from a single station. The positions of the four closest GCM gridpoints are also displayed in Fig. 1.

Fig. 1. Location of the catchments and four close ECHAM gridpoints

3. Downscaling Method

The method used is a multiple linear regression between principal components (PCs) of predictor field(s) as dependent variables, and local temperature/precipitation as the independent variable. Although the variance of a surface climate variable explained by a set of PCs is smaller than that explained by the original gridded data (even if a screening procedure is applied to the latter; Klein and Walsh, 1983; Huth, 1997), we prefer to use PCs because the ability of GCMs to simulate large-scale correlation/covariance structures is generally better relative to individual gridpoint values.

Principal components are calculated from monthly Z500 and TH anomalies, defined as departures from the corresponding 30-year monthly means. The procedure is similar to that employed by Barnston and Livezey (1987), which may be referred to for more information on principal component analysis (PCA). Separate PCs are calculated for seasons defined by a variety of groupings of months (see Sec. 5). Three sets of PCs are produced for each season: PCs of geopotential heights alone, PCs of thickness alone, and joint PCs, calculated from the two fields together. The data matrix thus consists of 63 columns (corresponding to 63 gridpoints) in the former two cases, and of 126 columns (two quantities for each gridpoint) in the latter case. A correlation matrix was used in the PCA. The PCs are orthogonally rotated using Varimax criterion, in order to make their interpretation possible while retaining the linear independence of PC scores (i.e., time series of PC amplitudes). To determine the number of PCs to be retained and rotated, we employ O'Lenic and Livezey's (1988) criterion of cutting the PCs just behind the last section of relatively small slope (shelf) in an eigenvalue vs. PC-number diagram, which has been shown to be suitable in identifying modes of circulation variability. In most cases, the criterion was easy to apply. The numbers of PCs retained differ among seasons and among predictor sets. For the commonly defined seasons (DJF, MAM, etc.), we retained 5 PCs for Z500 and 6 PCs for joint predictor (Z500 + TH) in all seasons. For TH, the number of retained PCs is 9 in summer and 6 in other seasons. The variance explained by the retained PCs is generally largest in winter (about 92%) and smallest in summer (about 80%), and differs by only a little amount (3% maximum) among the three PC sets.

If only Z500 PCs are taken as the predictors in the linear regression equation, all the PCs retained are used in the regression model, i.e., no screening is applied. The information on the thermal structure of the lower troposphere (the TH field) can be included in two ways: The regression can be based either on joint (Z500 + TH) PCs or on separate Z500 and TH PCs. In the former case, no screening is applied since all the PCs are linearly independent by definition. On the other hand, PCs of Z500 field and PCs of TH field are strongly interrelated and screening is therefore necessary.

The stepwise screening procedure is used, in which each potential predictor variable is evaluated for its individual significance level before including it in the equation, and, after each addition, each variable within the equation is evaluated for its significance as part of the model. The significance levels for entering variables into the equation and retaining them were set to 90% and 95%, respectively.

4. Validation

4.1 Surface Variables

A comparison of temperature and precipitation as simulated by the ECHAM3 GCM, with observations, in the two catchments, was performed in detail by Nemešová et al. (1998). Here we compare the annual cycles of monthly mean temperature and monthly precipitation for both catchments and the four closest GCM gridpoints (Fig. 2). The difference between the simulated and observed cycles is much greater than the spread of curves among gridpoints and between catchments. The control climate is warmer than the observed throughout the year except for spring. Temperatures peak later in summer: the annual maximum occurs in August instead of July. Annual precipitation is about twice as large in the control climate than the observed and the precipitation distribution during the year is entirely different.

Because of these deficiencies the simulation of neither temperature nor precipitation annual cycle can be considered satisfactory. The attempt to downscale both variables from large-scale upper-air fields is thus justified on this basis.

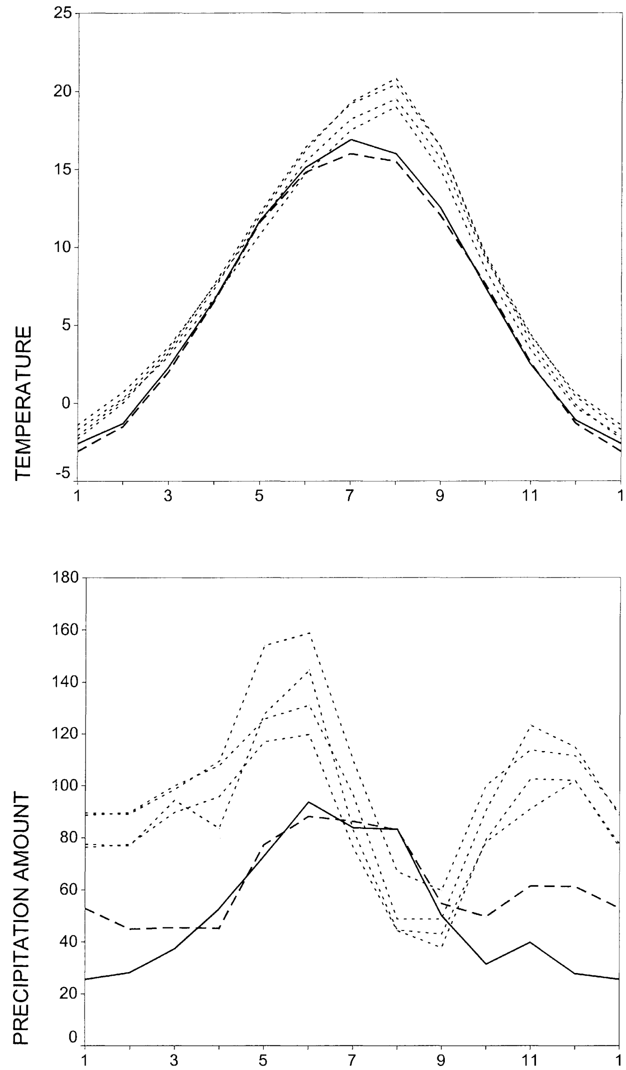

Fig. 2. Annual cycles of temperature (°C) and precipitation (mm) for the Blanice (solid line) and Metuje (dashed) catchments and at the four ECHAM gridpoints (dotted)

4.2 Upper-Air Fields

A simple comparison of annual mean 500 hPa heights and 1000/500 hPa thickness shows that the ECHAM GCM simulates the lower troposphere too warm and the 500 hPa level too high. The maximum bias is located over northwest France for both fields (not shown).

The percentage of variance explained by the eight leading PCs (modes of variability) of the three predictor sets (Z500, TH, joint) in winter (DJF) in the observations and the GCM control run is shown in Table 1. The number of PCs to be retained was determined according to O'Lenic and Livezey's (1988) criterion, described in the previous section. In the Z500 PCs, a drop in the explained variance occurs between the fifth and sixth PC in both climates, indicating that the number of relevant Z500 PCs, five, is the same. On the other hand, in both TH and joint PCs a drop occurs after the sixth PC in the observations, but after the fifth PC in the control climate. In addition to this, 5 PCs in the control run explain approximately the same amount of variance as 6 PCs in the observations. Both these findings indicate that there are only five relevant PCs in the control climate, not six as in the observations. The results are very similar in other seasons.

The maps of the Z500 and TH loadings (i.e., correlations between the gridpoint values and PC

Table 1. *Percentage of Variance Explained by 8 Leading PCs of 500 hPa Heights (Z500), Thickness (TH), and Joint PCs of Z500 and TH (Joint; for Definition see Text); for the Observed (OBS) and GCM Control (CTR) Climates; all for Winter (DJF). Cummulative Variance Explained by Leading 5 and 6 PCs (Denoted C5 and C6, Respectively) is Displayed in the Last Two Rows*

	Z500		RT		Joint	
PC	OBS	CTR	OBS	CTR	OBS	CTR
1	29.3	36.5	36.4	33.9	30.9	33.3
2	26.4	28.8	23.3	31.7	22.4	26.9
3	19.1	18.5	13.5	12.8	14.9	16.2
4	10.1	6.9	9.3	8.0	10.2	8.0
5	7.2	4.7	6.2	5.6	6.7	5.1
6	2.6	1.6	4.1	2.3	4.0	2.3
7	2.1	1.0	1.8	1.4	2.0	1.8
8	1.1	.7	1.4	1.1	1.5	1.2
C5	92.1	95.5	88.6	92.0	85.0	89.5
C6	94.7	97.1	92.1	94.2	89.1	91.8

scores) for DJF are compared between the observed and control climate in Figs. 3 and 4. There is a clear one-to-one correspondence between the observed and control PCs of the Z500 field (Fig. 3). The correspondence is underscored by the correlation between the loading patterns (Table 2): All the correlation coefficients between the corresponding patterns greatly exceed 0.9. For the TH field, several pairs of the observed and control PCs can also be found (Fig. 4): observed PCs 1, 4, 5 and 6 correspond in turn to control PCs 3, 4, 5 and 2. PC 2 in the observations manifests a weaker correspondence with the control PC 1 since its center is shifted ten degrees eastwards. However, observed PC 3 has no counterpart in the control climate. Pattern correlations (Table 3) confirm that the one-to-one correspondence is incomplete and observed mode 3 is not reproduced in the control climate. If only 5 PCs are rotated in the control climate, a one-to-one correspondence between the observed and control PCs appears except for the observed PC 3, which has no counterpart in the control climate (Table 4). This indicates that the variations in lower tropospheric temperature centered over Tunisia are not reproduced by the ECHAM3 GCM. The lower number of relevant TH PCs in the control climate, five, which is indicated by the percentage of variance in Table 1, is thus confirmed. A similar effect appears for the joint predictor: the observed PC with its Z500 and TH anomaly center over

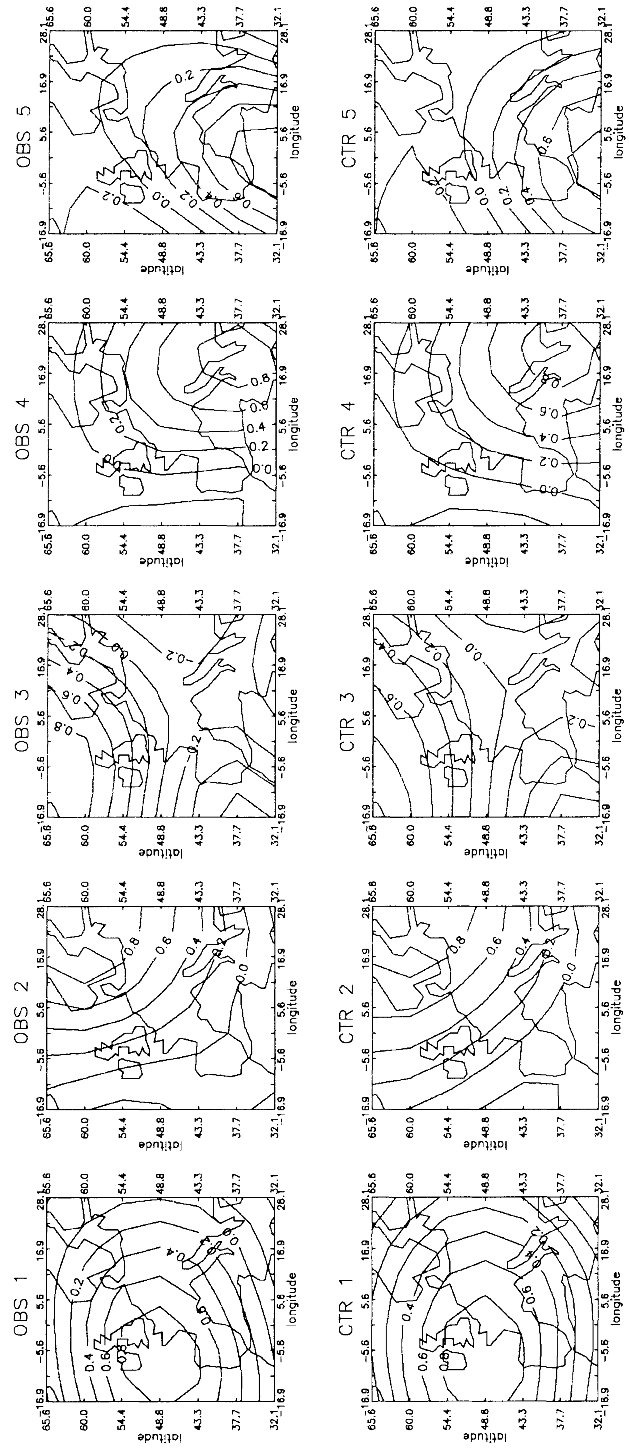

Fig. 3. Rotated PC loadings for 500 hPa heights in winter for a 5-PC solution: observed (top) and control run (bottom)

Tunisia is missing in the control climate (not shown).

In other seasons, the performance of the model is similar to that for winter: The control Z500 PCs correspond to the observed PCs quite closely,

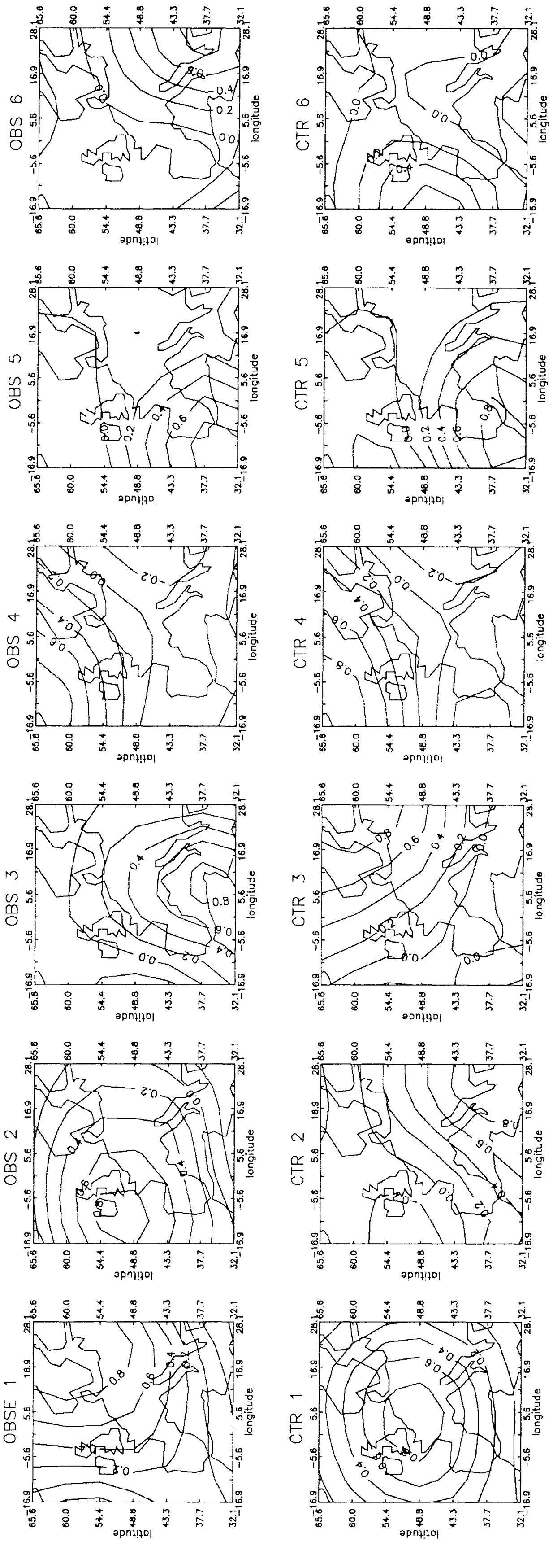

Fig. 4. Rotated PC loadings for thickness in winter for a 6-PC solution: observed (top) and control run (bottom)

Table 2. *Correlation Coefficients Between Five Observed and Control PC Loadings for 500 hPa Heights, Winter (DJF). One-to-one Correspondence is Indicated in Boldface*

		CONTROL				
	PC	1	2	3	4	5
OBSERVED	1	**.980**	−.196	−.121	−.294	−.047
	2	−.149	**.973**	.241	.000	−.464
	3	−.030	.287	**.978**	−.392	−.655
	4	−.199	.052	−.313	**.988**	.235
	5	.012	−.408	−.629	.311	**.934**

Table 3. *Same as in Table 2 Except for 6 PCs of Thickness*

		CONTROL					
	PC	1	2	3	4	5	6
OBSERVED	1	.427	−.381	**.916**	.165	−.404	−.108
	2	**.860**	−.573	−.105	.161	−.163	.770
	3	.066	.689	−.438	−.484	.655	−.521
	4	−.093	−.630	.077	**.972**	−.611	−.032
	5	−.060	.170	−.345	−.580	**.880**	.178
	6	−.291	**.890**	−.243	−.630	.186	−.228

Table 4. *Same as in Table 3 Except for 6 Observed PCs and 5 Control PCs*

		CONTROL				
	PC	1	2	3	4	5
OBSERVED	1	.265	−.359	**.953**	.186	−.371
	2	**.970**	−.514	−.042	.108	−.167
	3	−.116	.768	−.374	−.446	.617
	4	.005	−.636	.043	**.970**	−.603
	5	.005	.195	−.360	−.580	**.895**
	6	−.384	**.846**	−.232	−.629	.148

whereas the ECHAM GCM simulates fewer relevant thickness PCs than occur in the observations.

5. Downscaling of Observed Data

5.1 Selection of Predictors and Predictands

First of all, the optimum configuration of predictors and predictands is selected. More specifically, we examine the effect on the accuracy of the downscaled variables of (i) taking anomalies or raw values as predictands, (ii) including thickness among the predictors, and (iii) the way in which thickness is included. For this purpose, the downscaling procedure is applied to the whole 30-year period of observed data and based on standard seasons (winter is December to February etc.): principal components and regression coefficients are determined for each season separately. The evaluation is performed for seasons in terms of the squared correlation coefficient, i.e., the share of variance explained by the regression equation.

The results are presented in Fig. 5 for the Metuje catchment for both variables, in all four seasons, and with four configurations of predictors and predictands (regression methods). If principal components of Z500 field are used as the predictor, taking anomalies (method B) instead of raw values (method A) of the predictand variable improves the specification of temperature throughout the year, most notably in spring and autumn, whereas the improvement for precipitation is only marginal. The inclusion of thickness in the predictors (method C) further improves the specification of temperature. The results are better in all seasons for stepwise regression performed on PCs calculated for Z500 and TH fields separately (method D) than for regression of joint PCs without screening (method C). The inclusion of thickness does not lead to any improvement in the specification of precipitation.

The variance explained by circulation and lower tropospheric thickness using the best method (D) is much larger for temperature than for precipitation. For temperature, the variance explained is largest in spring, exceeding 80% at both stations, while smallest in autumn. Very low portions of the total variance of precipitation are explained, only exceeding one third for Metuje in winter. The worst results are obtained for the convective season (spring and summer).

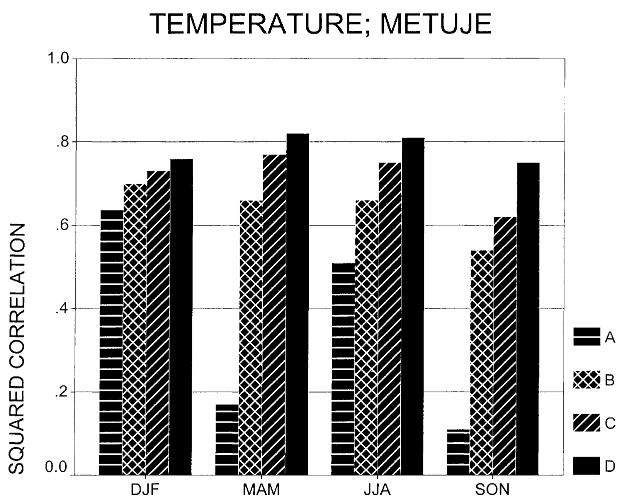

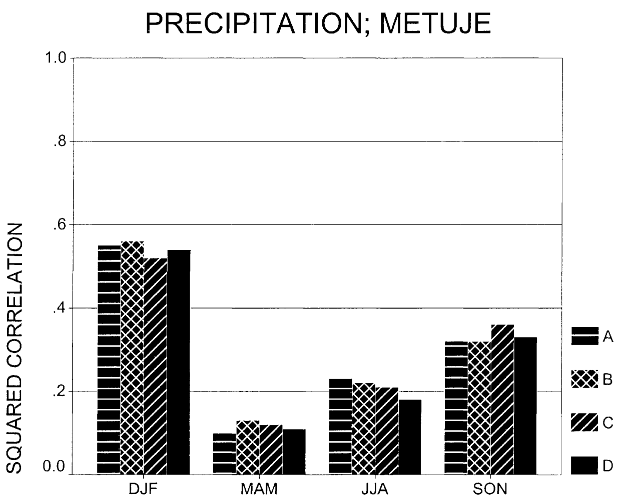

Fig. 5. Selection of predictors, Metuje; temperature (top) and precipitation (bottom). Shown are squared correlations between downscaled values and observations for the following predictors: PCs of raw 500 hPa heights (A); PCs of 500 hPa height anomalies (B); joint PCs of anomalies of 500 hPa heights and relative topography (C); PCs of 500 hPa anomalies and PCs of relative topography anomalies (D)

5.2 Definition of Seasons

In this subsection we attempt to find the optimum definition of seasons, that is, a definition for which the largest share of variance is explained. This is done using a cross-validation scheme, which provides an unbiased estimate of potential ‘predictability’ of temperature and precipitation. The cross-validation consists in omitting one season at a time, building the statistical model on the rest of data, and testing it on the omitted season as on an independent sample (Michaelsen, 1987). The accuracy of cross-validated temperature and precipitation is evaluated by correlating specified values with observations for each calendar month separately.

The selection of the optimum length of seasons for downscaling temperature is illustrated in Fig. 6. Three partitions of the year are considered: (i) the whole year treated as one season; (ii) four three-month seasons defined in a common way (winter as December to February, spring as March to May,

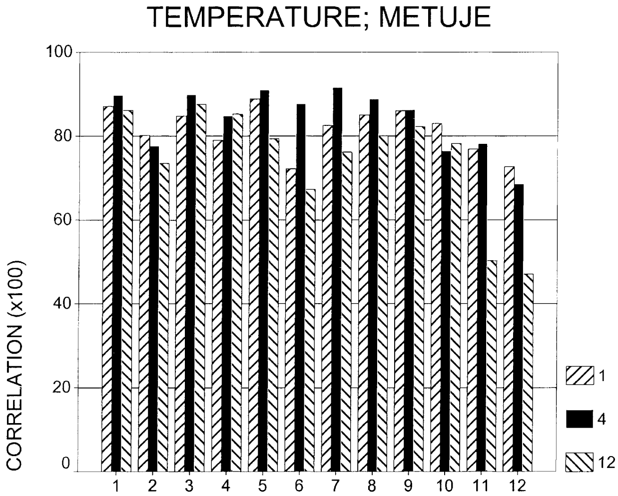

Fig. 6. Selection of the length of seasons for Metuje. Shown are correlations ($\times$ 100) between downscaled and observed temperatures for one season 12 months long (entire year; 1), four three-month seasons (4); 12 one-month seasons (each month separately; 12)

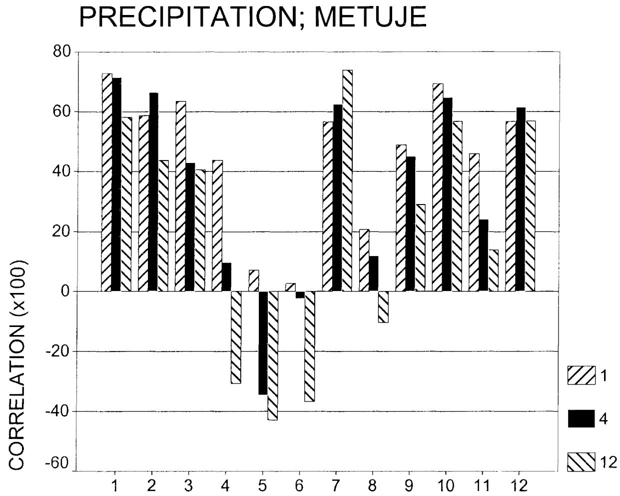

Fig. 7. Same as in Fig. 6, except for precipitation

etc.); and (iii) each month treated as a separate season. Building the regression model for each month separately (bars furthest to the right) yields the worst results, mainly in November and December. The overall performance appears to be best for the three-month seasons (black bars). The performance of the regression method peaks in the warm half of the year and is weakest in November and December in both catchments. There are three possible sets of three-month seasons: one starting with December to February (the ordinary definition), the second starting with January to March, and the third with February to April. There is a great deal of similarity in the level of performance among the sets of seasons, but the ordinary seasons (DJF, . . .), nevertheless, tend to produce the best results (not shown).

For precipitation, treating each month separately results in several negative correlations (Fig. 7). This outcome, however, is rather a common case in cross-validating regression 'forecasts' if the expected skill (in terms of correlation) is close to zero (Barnston and van den Dool, 1993). The three-month seasons tend to be better than the year as a whole from October to March in the Blanice catchment (not shown) but for three separate months only (February, July, December) in the Metuje catchment. In the warm half-year (April to September), the skill is low, indicating that the specification of precipitation fails in months when convective precipitation prevails. The only months when precipitation can be specified from circulation and thickness in both catchments with a reasonable skill are October, December, January and February.

Because of the low skill levels obtained for downscaling monthly precipitation, the rest of this study is confined to an analysis of temperature only.

5.3 *Analogue of a Warmer Climate*

Our ultimate aim is to apply the downscaling procedure to a future, likely warmer climate. Before doing that, it is useful to know if the method is transferable from one climate state (on which it is developed) to another and to what extent it can reproduce the difference between the two climate states. For this purpose, we applied the procedure similar to that used by von Storch et al. (1993): We selected the ten coldest and ten warmest seasons (winters, springs, etc.) from the observed dataset as an analogue of the difference between the present and future, likely warmer climate. The linear regression model was built on thirty monthly mean temperature anomalies of the ten coldest seasons, and then applied to thirty months of the ten warmest seasons as an independent sample.

The observed and downscaled temperatures in the ten warmest seasons are compared in terms of their mean anomaly (Fig. 8) and absolute range

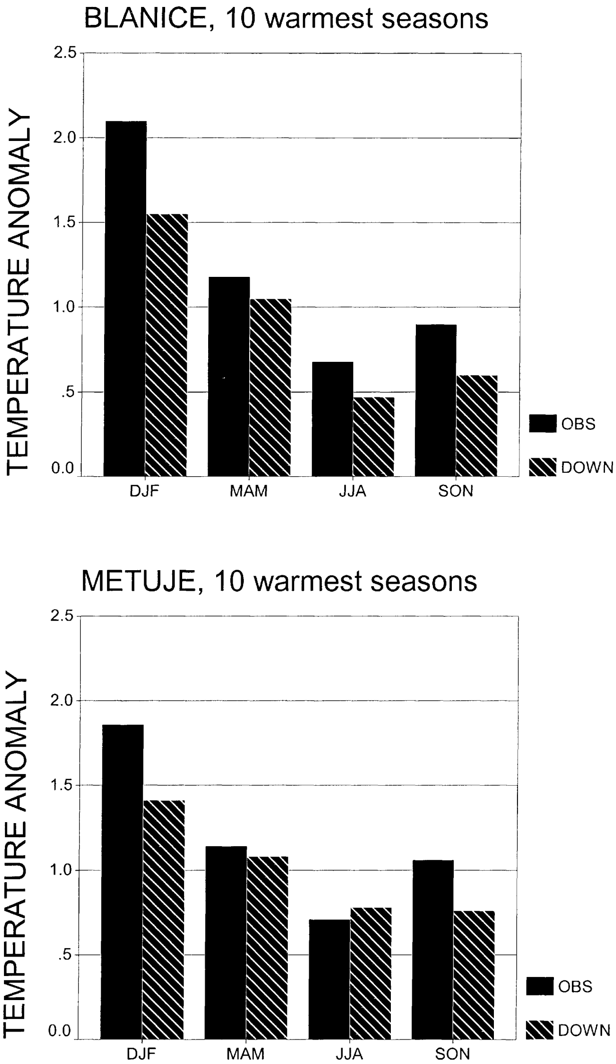

Fig. 8. Test on an independent sample. Mean temperature anomalies of ten warmest seasons in observations (OBS) and downscaled values defined by regression on ten coldest seasons (DOWN)

(i.e., the difference between the maximum and minimum monthly value; not shown). The downscaling method reproduces the positive anomaly of the warm seasons reasonably well, although it tends to underestimate the size of the anomaly throughout the year (except summer in the Metuje catchment). This is a consequence of the downscaled values having lower variance than the observed values. The difference between the warm and cold 'climate states' appears to be best captured in spring. The absolute range is reproduced well in all seasons except winter for which the downscaled temperatures are much more variable: the observed range for the Blanice catchment is 8 °C whereas in the downscaled values, it approaches 15 °C. A possible explanation for this is that in reality the direct effect of circulation is dampened by local influences, such as temperature inversions, inhibiting surface from excessive warming when warm advection occurs above. In the regression model, such damping effects are absent and warm advection can thus raise surface temperatures without any physical limitations.

The results show that the downscaling procedure is capable of capturing differences in mean temperatures between two climate states. It is, therefore, meaningful to apply the method to derive temperature scenarios for a warmer $2xCO_2$ climate.

6. Downscaling of GCM Data

6.1 Methodological Considerations

The downscaling method used in this study possesses three options when applied to GCM data: 1. Should the predictor anomalies be defined by subtracting from the observed or the control mean? 2. Should the predictand anomalies, i.e., the output from the regression equation, be added to the observed or the control mean? 3. Should the regression be based on PCs directly computed from the GCM control run, or on the projection of the observed PCs onto the control run? Similar questions apply to any statistical downscaling technique (e.g., canonical correlation analysis), but only a few studies explicitly mention which options are actually employed.

The first two options are twinned. Taking the anomalies from the control run as the predictors makes the anomalies downscaled from the control run have zero mean. Consequently, the anomalies downscaled from the $2xCO_2$ run are free of the model's bias. Therefore, the unbiased full time series for the $2xCO_2$ climate at a given site can be made up by adding downscaled anomalies to the observed mean. The appropriateness of this approach has been shown by Karl et al. (1990) and Winkler et al. (1997). There appears, however, to be an alternative: The observed mean can be subtracted from the GCM time series to produce anomalies. Then, the downscaled control anomalies no longer have zero mean and the downscaled $2xCO_2$ anomalies include the model's bias. The bias may be eliminated by subtracting the mean control anomaly from the downscaled $2xCO_2$ anomalies, the full $2xCO_2$ time series is then constructed by adding the observed mean. In this study we employ the former method of eliminating bias from the GCM downscaled series (hereafter referred to as 'C' method; C stands for control) because it is simpler and perhaps more intuitive. The latter method ('O' for observed) is used for comparison purposes only.

The advantage of using the model's own PCs (e.g., Hewitson, 1994) rather than the projections of the observed PCs can be seen in that the intrinsic PCs explain more variance in the GCM run than the projected ones. However, the necessary condition for control PCs to be used in the downscaling procedure is a one-to-one correspondence between the observed and control PCs. If the model fails to simulate the PCs with enough accuracy, the observed relationships with surface climate may not be valid in the control climate (for example, a poleward shift of a pattern like mode 1 in Fig. 4 would be connected with a flow that has a more northerly component, inducing advection of cooler air), or even impossible to apply if a relevant observed PC is absent in the control run. Since the latter situation is the case in this study (the observed PC of thickness centered over Tunisia is not reproduced in the control climate), we decided to project observed PCs onto both GCM climates, and to base the regression on these projections rather than on the GCM's intrinsic PCs.

6.2 *Application to GCM Output*

The monthly mean temperature anomalies corresponding to the present and $2xCO_2$ climates, obtained directly from GCM output and by the two downscaling methods (referred to above) for the Blanice catchment are presented in Table 5. The downscaling is based on commonly defined seasons. The mean of the downscaled control series is identical to the observed mean by definition if the C method is employed. The temperature bias of the control climate is larger for the O downscaling method than for direct GCM output. This points to the fact that the model does not correctly simulate the links between the large-scale and local-scale: If it did, the GCM's bias would originate from the large-scale bias only, as in O-downscaling, and the GCM's and the O-method biases would be close to each other. The resulting $2xCO_2$ anomalies (to be added to the observed means) are fairly similar for the two downscaling methods, and both differ considerably from the direct GCM output for most months (see the four rightmost columns in Table 5 for Blanice and Table 6 for Metuje). This means that the removal of the model's bias in the O downscaling method is almost as effective as in the simpler C method.

Table 5. *Temperature Anomalies in the Blanice Catchment for Control (CTR) and $2xCO_2$ (SCA) Climates, and Anticipated Warming (Difference SCA–CTR), for Direct ECHAM Output and two Downscaling Methods (O and C). In the Rightmost Column are Differences in Anticipated Warming Between the two Downscaling Methods (O–C). Downscaling Performed for Standard Seasons (DJF, MAM, etc.)*

	Temperature anomalies									diff.
	ECHAM		downscaling O		downscaling C		Anticipated warming			down
Month	CTR	SCA	CTR	SCA	CTR	SCA	ECHAM	down O	down C	O–C
1	.5	3.7	2.7	4.6	.0	1.4	3.2	1.9	1.4	.5
2	1.5	3.7	3.9	4.5	.0	.6	2.2	.6	.6	.0
3	.7	3.8	2.3	5.0	.0	2.6	3.1	2.7	2.6	.1
4	.0	3.3	1.3	4.2	.0	2.8	3.3	2.9	2.8	.1
5	−.8	1.8	.5	2.7	.0	2.1	2.6	2.2	2.1	.1
6	−.4	2.7	.7	1.5	.0	.7	3.1	.8	.7	.1
7	.7	6.0	1.1	2.6	.0	1.1	5.3	1.5	1.1	.4
8	3.0	9.6	1.6	3.5	.0	1.4	6.6	1.9	1.4	.5
9	2.4	7.0	2.9	8.4	.0	5.8	4.6	5.5	5.8	−.3
10	1.1	4.4	3.0	8.7	.0	5.9	3.3	5.7	5.9	−.2
11	1.0	3.2	4.1	8.8	.0	4.6	2.2	4.7	4.6	.1
12	.8	3.0	2.8	4.1	.0	1.0	2.2	1.3	1.0	.3

Table 6. *Anticipated Warming (Difference SCA–CTR) in the Metuje Catchment for Direct ECHAM Output and two Downscaling Methods (O and C). In the Rightmost Column are Differences of Anticipated Warming Between the two Downscaling Methods (O–C). Downscaling Performed for Standard Seasons (DJF, MAM, etc.)*

	Anticipated warming			diff. down
Month	ECHAM	down O	down C	O–C
1	2.7	.4	.3	.1
2	2.3	−.6	−.8	.2
3	3.1	2.4	2.4	.0
4	3.0	2.3	2.2	.1
5	2.3	1.3	1.3	.0
6	2.7	1.7	2.0	−.3
7	4.2	2.6	2.4	.2
8	5.4	2.8	2.7	.1
9	3.7	4.2	5.1	−.9
10	3.2	4.3	5.5	−1.2
11	2.4	4.0	4.7	−.7
12	2.1	−.2	−.2	.0

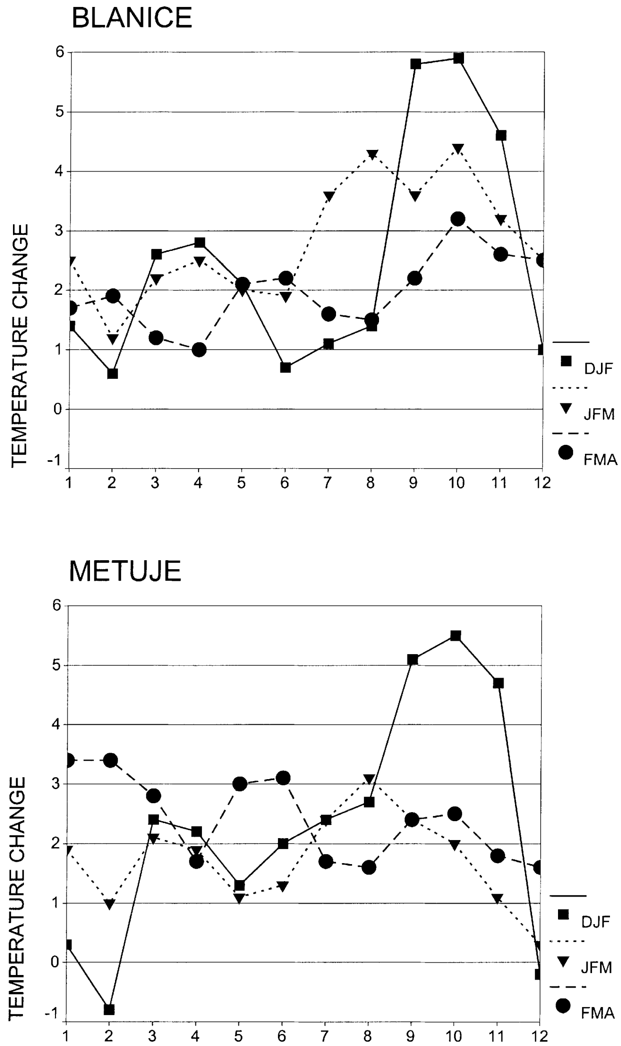

Fig. 9. Downscaled temperature change (difference between the $2x\mathrm{CO}_2$ and present climates) obtained by the C method for three sets of three-month seasons (starting with DJF, JFM and FMA)

Discontinuities may appear between seasons in the annual cycle of downscaled temperature change: In Tables 5 and 6 we can see that the autumn changes stand out from the summer and winter changes in both catchments for both downscaling methods. This is further illustrated in Fig. 9 where the annual cycles of the downscaled temperature change are shown for the C method and for three possible definitions of seasons. A similar, though smaller, discontinuity can be found e.g., between June and July for the JFM seasons in the Blanice catchment. The reason for such inconsistencies is that the predictors involved in the regression equation differ from season to season and the response of PCs' magnitudes to increased greenhouse forcing differs from one PC to another. Table 7 shows that in autumn, the predictors with a strong response enter the regression equation with mostly positive coefficients, causing a high warming rate. In neighbouring seasons, the predictors with smaller response dominate and/ or several predictors are included with a negative regression coefficient, thus damping the temperature response.

To minimize the effect of different predictors entering downscaling procedure in different seasons, we decided to construct the final annual cycle of monthly mean temperature response to doubled greenhouse forcing by averaging the three annual cycles based on the three definitions of seasons. The final downscaled temperature change is displayed in Fig. 10 together with the temperature scenario derived directly from the ECHAM GCM by subtracting gridpoint $2x\mathrm{CO}_2$ and control values. In general, downscaling produces less warming than the GCM itself, with the exception of October and November. The downscaled annual cycles differ from the GCM ones in that they indicate maximum warming in autumn (by 4.5 °C for Blanice and 3.3 °C for Metuje); minimum warming occurs in winter. A tendency towards a stronger downscaled temperature response is observed in the Blanice catchment, which is consistent with the

Table 7. *Response to Enhanced Greenhouse Effect (Difference SCA–CTR) in Mean Amplitude of PC Projections (Diff.) and Regression Coefficients for Blanice (Blan) and Metuje (Met). All for JJA, SON and DJF Seasons*

PC	JJA Diff.	Blan	Met	SON Diff.	Blan	Met	DJF Diff.	Blan	Met
Z1	.59	+.190	+.245	1.18	–	–	.00	+.590	+.589
Z2	1.92	–	+.253	.88	–	−.420	.49	−.845	−.837
Z3	2.78	−.318	–	.82	+.424	–	.58	−1.055	−.713
Z4	5.13	–	–	1.59	+.569	–	1.26	–	–
Z5	4.63	–	–	2.90	+.505	+.943	.95	+1.563	+1.049
TH1	.25	+.367	–	.77	–	+.998	.79	+1.316	+1.900
TH2	1.08	–	–	1.75	+.471	+.674	.15	–	+1.042
TH3	2.53	–	–	2.04	–	–	.80	–	–
TH4	1.40	–	–	3.58	–	–	1.92	–	–
TH5	2.99	–	–	3.25	+.582	+.631	2.62	−.673	−.792
TH6	1.10	+.511	+.322	1.89	–	−.669	2.24	+.644	–
TH7	1.81	+.507	+.447						
TH8	.89	+.341	+.655						
TH9	1.26	–	–						

direct GCM output, also yielding more warming for Blanice catchment.

The temperature scenarios, i.e., the annual cycles for the $2x\mathrm{CO}_2$ climate, obtained both by downscaling and directly from the GCM output, are shown in Fig. 11 for the two catchments. Also shown are annual cycles for the two representations of the present climate, viz., the observations (which are identical with the values downscaled from the control run) and the control GCM run. The downscaling retains the annual maximum in July in the $2x\mathrm{CO}_2$ climate as in the observations, unlike the ECHAM simulations which have an unrealistically late annual temperature maximum in August, which is even amplified in the GCM $2x\mathrm{CO}_2$ climate.

7. Conclusions

The ECHAM3 GCM simulates monthly mean temperatures and monthly precipitation totals in two catchments in the Czech Republic with considerable deficiencies. The potential for statistical downscaling from large-scale 500 hPa height and 1000/500 hPa thickness fields to provide their more accurate representation has therefore been examined. As a downscaling method, multiple linear regression of the principal components of the large-scale fields has been employed.

In general, downscaling is much more successful for temperature than precipitation. This is in accord with recent downscaling studies, carried out for different climatic conditions and based on various methodologies (Wilks, 1989; Wigley et al., 1990; Semenov and Barrow, 1997; Kidson and Thompson, 1998). Monthly precipitation in the two catchments can be specified from the large-scale circulation and thickness fields with reasonable accuracy in only a few single months particularly in the cold part of the year. In months when convective precipitation prevails, the percentage of precipitation variance explained rarely exceeds 20%, whatever configuration of predictors and seasons is used. This is consistent with results of Noguer (1994) who has shown precipitation downscaling to have virtually no skill over the Iberian Peninsula in summer. A possible improvement may be achieved by incorporating free-atmospheric moisture variables, such as specific humidity, into the predictors (as in Crane and Hewitson, 1998). These variables have not been used in regional validation studies yet, however, but they are likely to be simulated with less accuracy than circulation and free-atmospheric temperature. This may cause subsequent difficulties in applying observed humidity-to-precipitation relationships to GCM outputs. We do not expect much improvement if sea level pressure were used instead of mid-tropospheric geopotential heights because the success in specification of surface climate elements from circulation have been shown to be almost independent of whether SLP or upper air data is employed (Kidson, 1997).

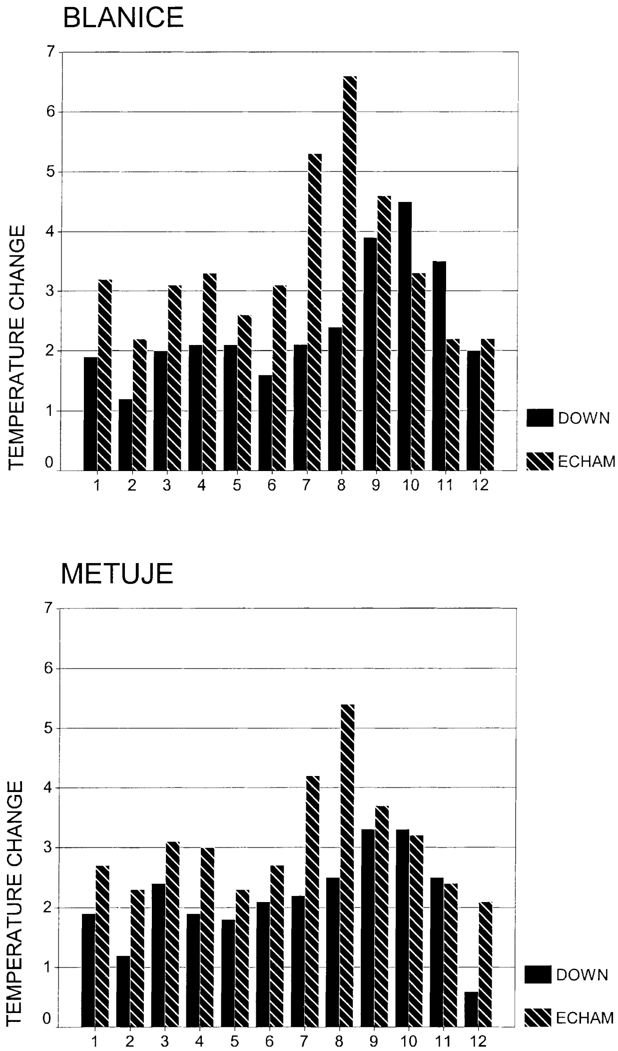

Fig. 10. Annual cycles of temperature change: obtained by averaging the three sets of downscaled temperature changes from Fig. 9 (DOWN); direct output from the model (ECHAM)

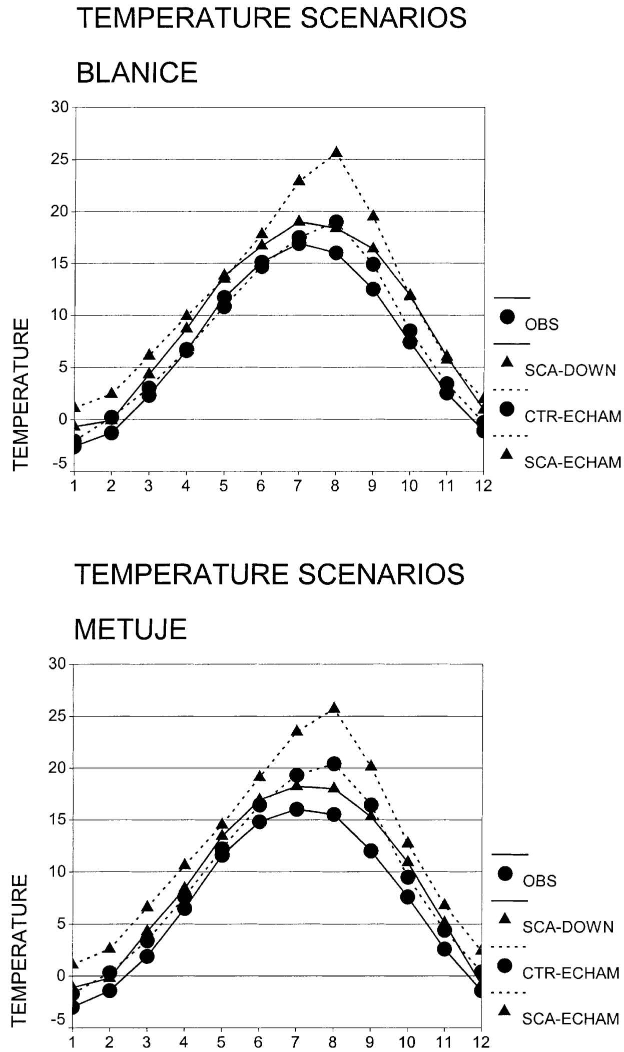

Fig. 11. Temperature annual cycles: observed (OBS), ECHAM control run (CTR-ECHAM), 2xCO$_2$ scenario from downscaling (SCA-DOWN), and 2xCO$_2$ scenario from the direct model output (SCA-ECHAM)

Another remedy is resorting to stochastic modelling techniques (weather generators), which has been proposed e.g., by Wilks (1989), Dubrovský (1997), and Semenov and Barrow (1997).

For downscaling temperature, the anomalies from the climatology are a better predictor than the raw data, especially in spring and autumn. The inclusion of large-scale free-atmospheric temperature among predictors leads to a pronounced improvement in the results, especially if principal components are calculated for circulation and temperature variables separately and stepwise screening is applied in the regression model. The optimum length of seasons appears to be three months; the three possible sets of three-month seasons yield comparable results, although the commonly defined seasons (starting with DJF) tend to be best. The correspondence of downscaled and observed temperatures is best in summer and lowest in late autumn and early winter. This reflects the fact that surface temperature in central Europe is more closely related to upper-air circulation in summer than in winter (Huth, 1997).

For constructing the climate change scenario, i.e., monthly mean temperatures for a 2xCO$_2$ climate, the outputs from the ECHAM3 GCM have been used. The procedure consists of four steps: first, the anomalies of predictor fields in the $2xCO_2$ GCM run are calculated from the climatology of the GCM control run; then they are projected onto the observed principal components. Third, regression models derived on observed data are applied to the projections to produce temperature anomalies in a $2xCO_2$ climate and finally, the anomalies are added to the observed climatology. Such a procedure allows the bias of the GCM to be reduced as much as possible. An alternative procedure that defines the $2xCO_2$ predictor anomalies by subtracting the observed climatology and constructs the $2xCO_2$ temperatures by adding the observed mean to the downscaling output and subtracting the mean control anomaly has been shown to yield similar results.

The final temperature scenario has been constructed by combining the three monthly $2xCO_2$ temperature series obtained by downscaling for three different definitions of seasons. The downscaled temperature response to an enhanced greenhouse effect is generally weaker than the response produced directly by the model. The maximum warming appears in October in both catchments, 4.5 °C for Blanice and 3.3 °C for Metuje, whereas the warming rate is smallest in winter. This is different from the scenarios for the Czech Republic based directly on outputs from the Global Institute for Space Studies (GISS) and Canadian Climate Centre (CCC) GCMs, which suggest more warming in winter than in summer (Kalvová and Nemešová, 1997). Higher warming rates in winter than in summer appear also in the majority of GCMs over southeastern and northeastern Europe (Kattenberg et al., 1996; Kittel et al., 1998). However, this should not be viewed as a discrepancy because on a regional scale, the range of winter and summer warming rates produced by various GCMs is quite large. Because of the uncertainties associated with the downscaled temperatures obtained in this study the results should be treated as one possible realization of many possible future climates rather than an actual prediction.

Acknowledgements

The authors thank to Dr. H. Österle, Institute for Climate Impact Studies, Potsdam, Dr. J. Buchtele, Institute of Hydrodynamics, Prague, and R. Schweitzer, University of Colorado, Boulder, for preparation and providing the datasets. The study was supported by the Grant Agency of the Czech Republic under contract 205/96/1670 and by the Grant Agency of the Academy of Sciences under contract A3060605.

References

Barnston, A. G., Livezey, R. E., 1987: Classification, seasonality and persistence of low-frequency atmospheric circulation patterns. *Mon. Wea. Rev.,* **115**, 1083–1126.

Barnston, A. G., van den Dool, H. M., 1993: A degeneracy in cross-validated skill in regression-based forecasts. *J. Climate,* **6**, 963–977.

Cavazos, T., 1997: Downscaling large-scale circulation to local winter rainfall in north-eastern Mexico. *Int. J. Climatol.,* **17**, 1069–1082.

Corte-Real, J., Zhang, X., Wang, X., 1995: Downscaling GCM information to regional scales: a non-parametric multivariate regression approach. *Clim. Dyn.,* **11**, 413–424.

Crane, R. G., Hewitson, B. C., 1998: Doubled CO_2 precipitation changes for the Susquehanna basin: Downscaling from the GENESIS general circulation model. *Int. J. Climatol.,* **18**, 65–76.

DKRZ, 1993: *The ECHAM3 Atmospheric General Circulation Model*. Report No. 6, Deutsches Klimarechenzentrum, Hamburg, 184 pp.

Dubrovský, M., 1997: Creating daily weather series with use of the weather generator. *Environmetrics,* **8**, 409–424.

Gates, W. L., Henderson-Sellers, A., Boer, G. J., Folland, C. K., Kitoh, A., McAvaney, B. J., Semazzi, F., Smith, N., Weaver, A. J., Zheng, Q.-C., 1996: Climate models – evaluation. In: Houghton, J. T., Meira Filho, L. G., Callander, B. A., Harris, N., Kattenberg, A., Maskell, K. (eds.) *Climate Change 1995. The Science of Climate Change*. Cambridge: Cambridge University Press, pp. 229–284.

Giorgi, F., Mearns, L. O., 1991: Approaches to the simulation of regional climate change: A review. *Rev. Geophys.,* **29**, 191–216.

Grotch, S. L., MacCracken, M. C., 1991: The use of general circulation models to predict regional climatic change. *J. Climate,* **4**, 286 – 303.

Hewitson, B., 1994: Regional climates in the GISS general circulation model: Surface air temperature. *J. Climate,* **7**, 283–303.

Huth, R., 1997: Potential of continental-scale circulation for the determination of local daily surface variables. *Theor. Appl. Climatol.,* **56**, 165–186.

Huth, R., 1999: Disaggregating climatic trends by classification of circulation patterns. *Int. J. Climatol.* (submitted).

Kaas, E., Frich, P., 1995: Diurnal temperature range and cloud cover in the Nordic countries: observed trends and estimates for the future. *Atmos. Res.,* **37**, 211–228.

Kalvová, J., Nemešová, I., 1997: Projections of climate change for the Czech Republic. *Clim. Change,* **36**, 41–64.

Karl, T. R., Wang, W. C., Schlesinger, M. E., Knight, R. W., Portman, D., 1990: A method of relating general circulation model simulated climate to the observed local climate. Part I: Seasonal statistics. *J. Climate,* **3**, 1053–1079.

Kattenberg, A., Giorgi, F., Grassl, H., Meehl, G. A., Mitchell, J. F. B., Stouffer, R. J., Tokioka, T., Weaver, A. J., Wigley, T. M. L., 1996: Climate models – projections of future climate. In: Houghton, J. T., Meira Filho, L. G., Callander, B. A., Harris, N., Katternberg, A., Maskell, K. (eds.) *Climate Change 1995. The Science of Climate Change*, Cambridge: Cambridge University Press, pp. 285–357.

Kidson, J. W., 1997: The utility of surface and upper air data in synoptic climatological specification of surface climatic variables. *Int. J. Climatol.,* **17**, 399–413.

Kidson, J. W., Thompson, C. S., 1998: A comparison of statistical and model-based downscaling techniques for estimating local climate variations. *J. Climate,* **11**, 735–753.

Kim, J. W., Chang, J. T., Baker, N. L., Wilks, D. S., Gates, W. L., 1984: The statistical problem of climate inversion: Determination of the relationship between local and large-scale climate. *Mon. Wea. Rev.,* **112**, 2069–2077.

Kittel, T. G. F., Giorgi, F., Meehl, G. A., 1998: Intercomparison of regional biases and doubled CO_2-sensitivity of coupled atmosphere-ocean general circulation model experiments. *Clim. Dyn.,* **14**, 1–15.

Klein, W. H., Walsh, J. E., 1983: A comparison of pointwise screening and empirical orthogonal functions is specifying monthly surface temperature from 700 mb data. *Mon. Wea. Rev.,* **111**, 669–673.

Michaelsen, J., 1987: Cross-validation in statistical climate forecast models. *J. Clim. Appl. Meteorol.,* **26**, 1589–1600.

Nemešová, I., Kalvová, J., Klimperová, N., Buchtele, J., 1998: Comparison of GCM-simulated and observed climates for assessing hydrological impacts of climate change. *J. Hydrol. Hydromech.,* **46**, 237–263.

Noguer, M., 1994: Using statistical techniques to deduce local climate distributions. An application for model validation. *Meteorol. Appl.,* **1**, 277–287.

O'Lenic, E. A., Livezey, R. E., 1988: Practical considerations in the use of rotated principal component analysis (RPCA) in diagnostic studies of upper-air height fields. *Mon. Wea. Rev.,* **116**, 1682–1689.

Palutikof, J. P., Winkler, J. A., Goodess, C. M., Andresen, J. A., 1997: The simulation of daily temperature time series from GCM output. Part I: Comparison of model data with observations. *J. Climate,* **10**, 2497–2513.

Schubert, S., Henderson-Sellers, A., 1997: A statistical model to downscale daily temperature extremes from synoptic-scale atmospheric circulation patterns in the Australian region. *Clim. Dyn.,* **13**, 223–234.

Semenov, M. A., Barrow, E. M., 1997: Use of a stochastic weather generator in the development of climate change scenarios. *Clim. Change,* **35**, 397–414.

von Storch, H., 1995: Inconsistencies at the interface of climate impact studies and global climate research. *Met. Zeitschrift, N.F.,* **4**, 72–80.

von Storch, H., Zorita, E., Cubasch, U., 1993: Downscaling of global climate change estimates to regional scales: An application to Iberian rainfall in wintertime. *J. Climate,* **6**, 1161–1171.

Wigley, T. M. L., Jones, P. D., Briffa, K. R., Smith, G., 1990: Obtaining sub-grid-scale information from coarse-resolution general circulation model output. *J. Geophys. Res.,* **95**, 1943–1953.

Wilks, D. S., 1989: Statistical specification of local surface weather elements from large-scale information. *Theor. Appl. Climatol.,* **40**, 119–134.

Winkler, J. A., Palutikof, J. P., Andresen, J. A., Goodess, C. M., 1997: The simulation of daily temperature time series from GCM output. Part II: Sensitivity analysis of an empirical transfer function methodology. *J. Climate,* **10**, 2514–2532.

Yarnal, B., 1985: A 500 mb synoptic climatology of Pacific north-west coast winters in relation to climatic variability, 1948–1949 to 1977–1978. *J. Climatol.,* **5**, 237–252.

Authors' address: Dr. Radan Huth, Jan Kyselý, Institute of Atmospheric Physics, Boční II 1401, 141 31 Praha 4, Czech Republic.